

Acoustic waves generated by a pulsed laser in anisotropic semiconductors

B. Audoin, H. Meri and C. Rossignol

Laboratoire de Mécanique Physique, UMR CNRS n° 5469,
Université Bordeaux 1, 33405 Talence, France, Email: b.audoin@lmp.u-bordeaux1.fr

Introduction

The volume contraction of a silicon crystal under intense illumination by laser light has been the motivation to study the ultrasound generation by the concentration-deformation mechanism [1]. More recently, the dynamics and kinetics of laser-induced plasma in semiconductors have been extensively explored to explain the influence of hot phonons on energy relaxation of dense electron-hole plasmas produced by laser pulses [2-4]. Numerous authors [5-6] have modelled the temperature rise and carrier concentration induced by laser pulse absorption on semiconductors. The effect of thermoelastic and electronic deformation contributions to the photoacoustic signals was experimentally and theoretically analysed. Experimentally, it was shown that [7] the shape of the acoustic pulses is dependent on the incident laser-energy density. The various thermoelastic and electronic deformation effects in semiconductors have been analysed by a coupled system of plasma, thermal and elastic equations. By using a 1D-coupled system, Gusev et al have shown that: the electronic deformation mechanism can contribute more than the thermoelastic mechanism to excited acoustic pulses [8-9]. Recently, The system of partially coupled plasma, thermal and elastic waves equations and conditions for neglecting the coupling between them have been quantitatively analysed for isotropic electronic, thermal and elastic properties, by Todorovic et al [10].

In this paper, we present a tow-dimensional (2D) model based on spatio-temporal Fourier transformations that allows us to describe the photo-thermic and photo-electronic generation of ultrasound by a laser line source in the case of an anisotropic sample.

Theoretical model

In our model, we consider an infinite plate of finite thickness h made of orthorhombic material. The coordinate axes x_1 , x_2 , and x_3 correspond to the principal axes of the medium, with x_1 being the optical axis of the incident laser radiation and assuming the line source is along the x_3 direction. Owing to the symmetry imposed by the source shape, the problem shows invariancy along direction x_3 .

To describe the laser generation of ultrasound in semiconductors, one must solve simultaneously the partially coupled plasma, thermal, and elastic waves equations. This theoretical model enables calculation of carrier density, $N(x_1, x_2, t)$, temperature, $T(x_1, x_2, t)$, and acoustic displacement vector, $\mathbf{u}(x_1, x_2, t)$ and describes their functional dependence to the thermal, elastic and carrier transport properties of the semiconductors.

The acoustic wave equation with an external force resulting from thermoelastic and electronic deformation mechanisms, is written as

$$\rho \frac{\partial^2 \mathbf{u}}{\partial t^2} - \nabla([C]:\nabla \mathbf{u}) = -[\lambda]\nabla T - [D]\nabla N \quad (1)$$

where ρ is the density, and $[C]$ is the stiffness tensor. $[\lambda]=[C]:[\alpha]$ is the stiffness-expansion tensor in witch $[\alpha]$ is the thermal expansion tensor of material. Additionnaly $[D]=[C]:[d]$ is the tensor of the difference in deformation potential of the conduction and valence bands in witch $[d]$ is the tensor of the pressure derivative of the energy gap (E_g).

The plasma equation describing the rise in carrier density N , is given by

$$\frac{\partial N}{\partial t} - \nabla([\Lambda]:\nabla N) + \frac{1}{\tau_R} N = \frac{Q(x_1, x_2, t)}{E} \quad (2)$$

Here $[\Lambda]$ is the ambipolar (carrier) diffusion tensor, $E = \hbar\omega$ the photon energy, and τ_R the Auger recombination time ($\propto 1/N^2$). The source term $Q(x_1, x_2, t)$ is dictated by the absorption of laser light

$$Q(x_1, x_2, t) = \beta I (1 - R) g(x_2) f(t) e^{-\beta x_1} \quad (3)$$

where β is the optical absorption coefficient, I is the energy incident by unit of length, and R is the optical reflectivity. $g(x_2)$ and $f(t)$ represent, respectively, the normalized linear and time distributions of the line source radiation. The structure of expression (3) indicates that: $Q \propto I$, whereas in equation (2) the inverse of the Auger recombination time $1/\tau_R \propto I^2$.

When the recombination of electron-hole pairs is considered, the fraction $(E - E_g)/E$ of the absorbed optical energy is thermalized. In this case the heat equation is

$$\rho C_p \frac{\partial T}{\partial t} - \nabla([\kappa]:\nabla T) = \frac{E - E_g}{E} Q(x_1, x_2, t) + \frac{E_g}{\tau_R} N \quad (4)$$

where $[\kappa]$ is the thermal conductivity tensor, and C_p the specific heat. The last term on the right-hand side of equation (4) describes crystal heating from the energy released by carrier recombination during Auger time.

At the surface $x_1=0$, the boundary conditions for the plasma density and temperature flows are

$$\Lambda_1 \frac{\partial N}{\partial x_1} = -\frac{\kappa_1}{E_g} \frac{\partial T}{\partial x_1} = SN \quad (5)$$

where S is the surface recombination velocity, which depends on surface conditions.

The set of equations (1), (2) and (4) is solved using spatio-temporal Fourier transformations. Applying these transforms yields a set of linear partial derivative equations with respect to the depth x_1 only. The solution is composed of a sum of exponential functions of x_1 . The displacement u at a given position and time is obtained by numerical inversions of the spatio-temporal Fourier transformations of the solution \tilde{u} calculated in the (k_2, ω) Fourier space.

Comparison with experimental results

The model is now used to calculate the normal component of the displacement for off-epicentre position.

A Nd:Yag laser producing various energy density pulses with a pulse duration of 20 ns, was used to generate the ultrasound in single-crystal silicon Si. The normal surface displacements associated with an ultrasonic arrival were detected on the opposite side of the excitation using a mach-Zehnder interferometer.

The signals for the Si sample were calculated for the following parameters: thickness $h=5$ mm; $\rho=2,332$ g.cm⁻³; $\alpha_{ii}=1,2 \times 10^{-5}$ K⁻¹; $C_p=757$ J.Kg⁻¹.K⁻¹; $\kappa_{ii}=150$ W.m⁻¹.K⁻¹; Optical absorption coefficient $\beta=1,43$ mm⁻¹ and optical reflectivity $R=0,3$ at $\lambda=1064$ nm; $\Lambda_{ii}=35$ cm².s⁻¹; $d_{ii}=-9 \times 10^{-22}$ mm³; $S=100$ m.s⁻¹; $E=1,17$ eV, $E_g=1,11$ eV; $C_{11}=C_{22}=194,36$ GPa, $C_{66}=50,90$ GPa and $C_{12}=35,24$ GPa. Two levels of linear incident energy density are adjusted: low $I_1=50,05$ mJ.mm⁻¹ and high $I_2=3,5$ mJ.mm⁻¹. The initially excited plasmas are for these two levels $N_{01}=2,5 \times 10^{15}$ mm⁻³ and $N_{02}=1,8 \times 10^{17}$ mm⁻³; respectively, so the corresponding Auger recombination times are $\tau_{R1}=0,38$ μ s and $\tau_{R2}=7,8 \times 10^{-5}$ μ s, respectively. The results for an off-epicentre position located by an angle of 35,7° (angle between the normal to the surface and the source-detection direction), are shown in Figures 1 and 2 for the low and high energies.

The comparisons between experiments and calculations shown in Fig 1-2 are excellent. Owing to the optical penetration, buried sources of contraction radiate longitudinal waves directly to the opposite interface. Their successive arrivals cause the first decrease before (L). The predominance of the contraction sources ($d_{ij}<0$) with respect to expansion sources ($\alpha_{ij}>0$) demonstrates that the main generation process is non thermal, see eq. (1), for silicon at 1064 nm. Following, waves, after (L) are waves generated by the buried contraction sources that have undergone reflection at the free upper interface. They arrive at the detector with a phase shift of π . They cause the signal increase after (L). Also very noticeable is the arrival (D) of waves resulting of internal diffraction. These waves are the signature of transient divergent waves in anisotropic media. Waves having undergone several reflections at the interfaces are also accurately represented by our calculations.

When the laser intensity increases, the term N/τ_R in Eq. 2 plays an important role and the carriers density N tends to decrease very rapidly with x_1 [8]. The sources then tend to be localised onto the surface. For these reasons, the peaks shape turns from monopolar, Fig. 1, to dipolar, Fig. 2, [7].

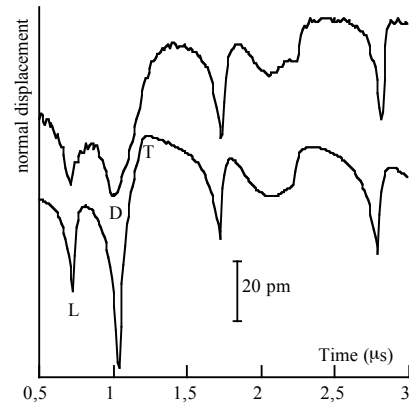


Figure 1: Experimental (top) and calculated (down) normal displacements associated with the low linear incident energy density $I_1=0,05$ mJ.mm⁻¹ for an off-epicentre position.

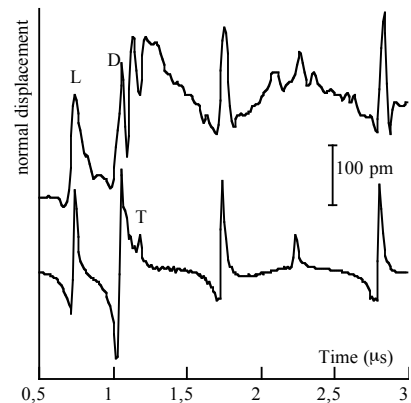


Figure 2: Experimental (top) and calculated (down) normal displacements associated with the high linear incident energy density $I_2=3,5$ mJ.mm⁻¹ for an off-epicentre position.

References

- [1] W. B. Gauster and D. H. Habing, Phys. Rev. Lett. **18** (1967), 1058-1061
- [2] E. J. Yoffa, Phys. Rev. B **21** (1980), 2415-2425
- [3] J. R. Goldman and J. A. Prybyla, Phys. Rev. Lett. **72** (1994), 1364-1367
- [4] H. M. Driel, Chemical physics **251** (2000), 309-318
- [5] A; Lietoila and J. F. Gibbons, J. Appl. Phys. **53** (1982), 3207-3213
- [6] L. Villegas-Lelovsky, G. Gonzalez de la Cruz, Y. G. Gurevich and I. N. Volvichev, Rev. sci. Instrum. **74** (2003), 556-558
- [7] S. Dixon, C. Edwards S. B. Palmers and D. W. Schindel, J. Phys D: Appl. Phys. **29** (1996), 1345-1348
- [8] V. E. Gusev and A. A. Karabutov, *Laser Optoacoustics*, AIP, Woodbury, NewYork, 1993
- [9] O. B. Wright and V. E. Gusev, Appl. Phys. Lett. **66** (1995), 1190-1192
- [10] D. M. Todorovic, Rev. sci. Instrum. **74** (2003), 582-585